DENTAL MATERIALS 35 (2019) 543–553

Available online at www.sciencedirect.com

ScienceDirect

journal homepage: www.intl.elsevierhealth.com/journals/dema

Effectiveness of pre-silanization in improving bond performance of universal adhesives or self-adhesive resin cements to silica-based ceramics: Chemical and *in vitro* evidences

Bingzhuo Chen[a,1], *Zhicen Lu*[a,1], *Hongliang Meng*[a], *Ying Chen*[a], *Lu Yang*[a], *Huaiqin Zhang*[a], *Haifeng Xie*[a,*], *Chen Chen*[b,*]

[a] *Jiangsu Key Laboratory of Oral Diseases, Nanjing Medical University, Department of Prosthodontics, Affiliated Hospital of Stomatology, Nanjing Medical University, Nanjing, China*

[b] *Jiangsu Key Laboratory of Oral Diseases, Nanjing Medical University, Department of Endodontics, Affiliated Hospital of Stomatology, Nanjing Medical University, Nanjing, China*

ARTICLE INFO

Article history:
Received 15 June 2018
Received in revised form
14 November 2018
Accepted 11 January 2019

Keywords:
Lithium disilicate
Silica-based ceramic
Silane
γ-MPS
Bonding
Thermodynamics calculations
Shear bond strength
Primer

ABSTRACT

Objectives. To examine effectiveness of pre-silanization in improving bond performance of multipurpose products such as universal adhesives or self-adhesive resin cements to silica-based ceramics.

Methods. The present study investigated reactions between silanol groups of γ-methacryloxypropyltrimethoxysilane (γ-MPS) and silica, dehydration self-condensation of γ-MPS, and condensation polymerization between γ-MPS and 10-methacryloyloxydecyl dihydrogen phosphate (10-MDP) by using thermodynamic calculations. Shear bond strength (SBS) tests were used to evaluate the influence of pre-silanization on resin bonding when a silane-containing universal adhesive, a silane-unknown universal adhesive, or two self-adhesive resin cements were applied for bonding lithium disilicate to resin. In addition, reactions between silane and lithium disilicate were analyzed using X-ray photoelectric spectroscopy (XPS) and Fourier transform infrared spectroscopy (FTIR).

Results. Acquired thermodynamic data indicated formation of siloxane between γ-MPS and silica. However, self-condensation of γ-MPS and reaction between γ-MPS and 10-MDP consumed the silanol. Pre-silanization enhanced SBS for self-adhesive resin cements or universal adhesives when applied for bonding silica-based ceramics. Thermocycling and aging decreased SBS in most groups. XPS and FTIR supported formation of siloxane between the employed silane coupling agent and two universal adhesives and lithium disilicate.

Significance. Pre-silanization is beneficial in further enhancing bond performance of universal adhesives or self-adhesive resin cements to silica-based ceramics.

* *Corresponding authors at*: Han Zhong Road 136th, Stomatological Hospital of Jiangsu Province, Nanjing 210029, China.
E-mail addresses: xhf-1980@126.com (H. Xie), ccchicy@njmu.edu.cn (C. Chen).

[1] These authors contributed equally to this work.

https://doi.org/10.1016/j.dental.2019.01.010

1. Introduction

Because of brittleness, silica-based ceramics only obtain enough resistance against biting and chewing after cementing on tooth abutments [1]. Silanization is nowadays the preferred chemical bonding strategy for silica-based ceramics, mediating the adhesion between silica in ceramic and resin matrix through formation of a siloxane (—Si—O—Si—) network on ceramic surface [2]. Among available functional silane monomers, γ-methacryloxypropyltrimethoxysilane (γ-MPS) is the most commonly used one. Despite its application for over 40 years, no novel monomers have replaced silanization to date [3]. Alternatively, when developing novel bonding systems, manufacturers aim to simplify clinical procedures, improve user friendliness, and reduce technology sensitivity of the processes. Fortunately, rapid technical innovation has endowed manufacturers to embrace versatile elements in designing multipurpose products without compromising bonding effectiveness, which also replaces multiple steps such as etching, priming, conditioning, and even cementing by lesser steps when cementing silica-based ceramic restorations to tooth abutments. At present, the development of multipurpose, all-in-one, and one-step bonding strategy is rapidly advancing.

The highly effective coupling of silane bases with activation and hydrolysis of silane in an aqueous environment generates free silanol groups [4]. These silanol groups undergo time-dependent dehydration and self-condensation, forming siloxane oligomers with temperature-, solvent system-, or pH-dependent sizes that can no longer bond to silica [4,5]. The optimum time period for silanization is supposed to be after hydrolysis and before oligomerization. For example, researchers who attempted to add extra silane into universal adhesives found that fresh mixtures can improve bond strength, while delayed application after 1, 3, or 7 days resulted in significantly lower bond strength [6]. More recently, a study provided Fourier transform infrared spectroscopy (FTIR) and nuclear magnetic resonance (NMR) spectroscopy evidences of dehydration self-condensation of silanol groups when γ-MPS was stored at pH < 3 for 10 days [7]. The hydrolysis step of silane to silanol groups was reported as a fast and reversible protonation of the alkoxy group of silane at an approximate pH of 4 [4]. However, multipurpose products including universal adhesives and self-adhesive resin cements also contain certain acidic functional monomers, such as 10-methacryloxydecyl dihydrogen phosphate (10-MDP), apart from silane, with the purpose of providing chemical affinity to dentin and metal oxides without pre-priming, which, in turn, usually results in a low-pH environment (pH < 3).

On account of advancement in technology, 10-MDP, silane, and other functional components can be retained as active in one bottle for a long time, and several *in vivo* bond test results have supported bond effectiveness of using these multipurpose products alone for bonding silica-based ceramics [8–10], instead of presenting with instability as observed with self-made mixtures in certain *in vivo* studies [6,7], dehydration self-condensation of silanol groups has been restrained in such multipurpose products. Recent studies have found that pre-silanization can further improve resin bond strength of silica-based ceramics when universal adhesives or self-adhesive resin cements are used [3,8]. Interestingly, in certain studies, no silanol groups were traced in silane- and 10-MDP-containing universal adhesives; the authors stated that mixing hydrolyzed silanes with 10-MDP deactivated the silanol groups via condensation reactions with hydroxyl groups of 10-MDP [6,11], wherein a possible hydrolyzable intermediate, Si—O—P, formed [12], which differs from dehydration self-condensation of silanol groups that deactivate silanol groups. Therefore, we have to consider the relationship of reactions between silanol groups in silane-containing multipurpose products and silica and that within these silane- and 10-MDP-containing multipurpose products, the dehydration self-condensation between the silanol groups, and the condensation polymerization between silanol groups and 10-MDP as well as their final influence on bond strength and bond duration of silica-based ceramics. The results would be helpful in analyzing whether pre-silanization in fact improves bond strength of silica-based ceramics further when using multipurpose products and to provide a definite answer regarding the need for pre-silanization when multipurpose products are used to bond silica-based ceramics.

Therefore, the present study aimed to analyze these reactions by using thermodynamic calculations and analytical characterizations with X-ray photoelectric spectroscopy (XPS) and FTIR. Furthermore, by means of shear bond strength (SBS) tests, we evaluated effectiveness of pre-silanization on bond strength and durability of silica-based ceramics when using universal adhesives or self-adhesive resin cements. The null hypotheses tested were (i) the silanol groups in silane undergo dehydration self-condensation (ii) and condensation with 10-MDP, which deactivates the silanol groups, and (iii) therefore, pre-silanization can further improve resin bonding of multipurpose products such as universal adhesives or self-adhesive resin cements when used for silica-based ceramics.

2. Methods and materials

2.1. *Modeling and thermodynamic calculations*

2.1.1. *Modeling of γ-MPS and SiO_2 clusters*

Based on the Inorganic Crystal Structure Database (ICSD; Fachinformationszentrum Karlsruhe Information Services, Eggenstein-Leopoldshafen, Germany), silicon dioxide (SiO_2) crystals were built. After building the SiO_2 crystal model, certain low index faces were cleaved by design to expose oxygen (O) atoms at the top of the faces in order to study atom arrangement. This also allowed us to note possible bonding sites for γ-MPS molecules on those faces as γ-MPS reacts with hydroxyl groups on the SiO_2 surface. In order to build the SiO_2 cluster so that it could be used for subsequent calculations, a small, neutral, repetitive unit was cleaved in the most common SiO_2 crystal structure. These "ideal" SiO_2 clusters should possess most features of SiO_2 crystals: (i) it is an electro-neutral MOX cluster; (ii) it is a repetitive unit of SiO_2 crystals; and (iii) the cluster size is appropriate for high-level ab initio calculation. Bonding between γ-MPS and SiO_2 clusters were calculated using high-level calculation. The density functional theory (DFT) along with the hybrid exchange functional of Becke's 3

parameters (B3) and the Lee–Yang–Parr's nonlocal correlation functional (LYP) were used to find stable optimization geometries and calculate thermodynamic functions of γ-MPS and the SiO_2 cluster. The basis sets for carbon (C), silicon (Si), O, and H were 6–311 + G** with polarization functions for C, Si, O, and H and with a diffuse function alone for C, Si, and O atoms.

2.1.2. *Complex of γ-MPS and SiO_2 clusters*

Interactions between γ-MPS and SiO_2 clusters were analyzed using thermodynamic calculations to examine stability of the complex of γ-MPS and SiO_2 clusters. Two or three hydroxyls were simulated to be replaced in γ-MPS depending on whether it was incomplete or totally hydrolyzed before being conditioned with SiO_2. Calculations were performed using the DFT/B3LYP method. The solvent effect was considered using the integral equation formalism polarizable continuum model (IEF-PCM).

2.1.3. *Hydrolysis and self-condensation of γ-MPS*

Water induces hydrolysis of the silane to give the corresponding silanol derivative. This silanol derivative then condenses with each other and with alkoxy groups, forming dimeric and oligomeric structures with further condensation [13]. The silanol produced and the dimeric of condensation of silanol groups were built according to their structures. Optimization geometries and frequency calculations were performed using the DFT/B3LYP method, and the basic sets were 6–311 + G**. Hydrolysis and condensation of γ-MPS were both simulated in the water phase. The solvent effect was considered using IEF-PCM.

2.1.4. *Complex of γ-MPS and 10-MDP*

The γ-MPS molecule was hydrolyzed in water and then supposed to be combined with 10-MDP. The structure of 10-MDP was built according to an earlier research, and the model of silanol was the same as mentioned earlier [14]. The complex of γ-MPS and 10-MDP was geometrically optimized, frequency calculations were performed. The DFT/B3LYP method was employed, and basic sets for C, H, O, and Si were 6–311 + G**, and polarization and diffusion functions were considered for the phosphorus (P) atom in 10-MDP. All reactions were simulated in the solvent so that calculations were finished in the water phase. The solvent effect was considered using IEF-PCM.

All calculations regarding geometrical optimization and thermodynamic functional calculations were performed using a Gaussian 09 software package (Gaussian, Wallingford, CT, USA). All data were calculated under standard conditions (1 atmosphere, 298 K). As translation entropy could not always be appropriately estimated, we eliminated the contribution of this part in order to enhance accuracy while calculating the sum of electronic and thermal free energies.

2.2. *SBS test*

Lithium disilicate blocks (e.max CAD, Ivoclar Vivadent, Amherst, NY, USA) in the bisque (blue, metasilicate) form were sectioned into $10 \times 10 \times 3\,mm^3$ plates by using a low-speed cutting device (Isomet, Buehler Ltd, Lake Bluff, IL, USA). The bonding surface of all plates were wet polished with 600, 800, and 1000 grit in order, by using a rotational polishing device (PG-1, BiaoYu instrument, ShangHai, China) and then sintered according to the recommended protocol. All specimens were etched with 9.5% hydrofluoric acid (HF; Porcelain etchant, Bisco) for 20 s, washed for 60 s, and subsequently dried after an ultrasonic bath for 5 min.

In total, 300 etched ceramic plates were prepared and were randomly assigned to 10 groups (n = 30) to receive the following surface conditioning:

Groups 1, 4 and 5, no further surface treatment;

Group 2, a coat of multipurpose universal adhesive, Single Bond Universal (3M ESPE), was applied to the etched surface and allowed to react for 15–20 s. The ceramic plate was air-dried to remove excess solvent, and was then light-cured for 10 s;

Group 3, procedures described in Group 2 was repeated, with the adhesive replaced by All Bond Universal (Bisco, USA).

Groups 6, 9 and 10, a coat of silane coupling agent (Porcelain Primer, Bisco, USA) was applied to the etched surface to react for 60 s, and then air dried;

Group 7, a coat of silane coupling agent was applied and then applied Single Bond Universal as in Group 2;

Group 8, a coat of silane coupling agent was applied and then applied All Bond Universal as in Group 3.

A tape with a 6 mm diameter hole was placed on the pre-treated ceramic surface to standardize the area for adhesion. Each resin cylinder was cemented onto the pre-treated ceramic plate by using a layer of composite resin cement under a constant load of 20 N. In the group 1, 2, 3, 6, 7 and 8, the conventional resin cement RelyX Veneer (3M ESPE, USA) was used. In group 4 and group 9, a self-adhesive resin cement, Clearfil SA Luting (Kuraray, Japan), was used for cementation. Another self-adhesive resin cement, RelyX Unicem (3M ESPE, Germany), was used in group 5 and group 10.

The tape was carefully removed after polymerization.

The universal adhesives and resin cements used, and details of treatments of each group are described in Table 1.

Half of the above prepared bonded specimens for each group were stored in distilled water at 37 °C for 24 h and the other half were submitted to artificial aging by 20,000 × thermocycling (TC-501F, Suzhou Weier Lab ware Co. Ltd., China) between two water baths of 5 °C and 55 °C with a dwell time of 30 s at each temperature and followed by 120 days of distilled water storage at 37 °C.

All bonded specimens were then subjected to an SBS test at a crosshead speed of 1.0 mm/min by using a universal testing machine (Instron Model 3365, ElectroPuls, MA, USA). The SBS value in MPa was calculated after satisfying normality and homogeneity of variance assumptions of data sets; means for each group were submitted to two-way analysis of variance (ANOVA) and post-hoc test to examine the influence of the surface treatments and aging. The aforementioned statistical analyses were performed using the SPSS 22.0 statistical software (SPSS Inc., Chicago, IL, USA). Statistical significance was preset at $\alpha = 0.05$. Fracture modes were classified as adhesive failures, fracture sites entirely located between the resin/cement and the zirconia surface; cohesive failures, fractures that exclusively occurred within the resin/cement; or mixed failures, partial resin/resin cement fractures and partial lithium disilicate plate surface exposure.

Table 1 – Surface treatment details for all experimental groups.

Groups	Surface treatment	Adhesives or resin cements
1	Immersion in 9.5% HF (Porcelain etchant, Bisco Inc., USA) for 20 s	RelyX Veneer (3M ESPE,USA) was applied to the ceramic surface to cement the pre-polymerized resin cylinders.
2		A coat of Single Bond Universal (3M ESPE, Germany) was applied to the ceramic surface and allowed to react for 15–20 s. The ceramic plate was air dried to remove excess solvent. The adhesive was light cured for 10 s. RelyX Veneer (3M ESPE, USA) was used as mentioned earlier.
3		A coat of All Bond Universal (Bisco Inc.,USA) was applied using the same procedure as mentioned earlier for Single Bond Universal. RelyX Veneer (3 M ESPE,USA) was used as mentioned earlier.
4		A coat of Clearfil SA Luting (Kuraray Noritake Medical Inc., Japan) was applied to the ceramic surface to cement the pre-polymerized resin cylinders.
5		A coat of RelyX Unicem (3M ESPE, Germany) was applied to the ceramic surface as mentioned earlier for Clearfil SA Luting.
6	Immersion in HF for 20 s, a coat of silane primer (Procelain Primer Bisco) was applied to the etched surface for 60 s and air dried for 10 s	RelyX Veneer (3M ESPE, USA) was used as mentioned earlier.
7		Application of Single Bond Universal and RelyX Veneer as mentioned earlier.
8		Application of All Bond Universal and RelyX Veneer as mentioned earlier
9		Application of Clearfil SA Luting as mentioned earlier
10		Application of RelyX Unicem as mentioned earlier

Table 2 – Details of the used materials in shear bond strength test and chemical characterization.

Material/Trade name	Main composition	Lot	Manufacture
IPS e.max CAD	SiO_2(57%–80%), Li_2O(11%–19%), K_2O(0%–13%), P_2O_5(0%–11%), ZrO_2(0%–8%), ZnO(0%–8%), Al_2O_3(0%–5%), MgO(0%–5%), pigments(0%–8%)	W43261 W88631 W41325 W85659 W89815	Ivoclar Vivadent, Schaan, Liechtenstein
Light-polymerized resin cement/RelyX Veneer	TEGDMA, Bis-GMA, 66 wt.% (47vol%) zirconia/silica	N862243	3M ESPE, MN, USA
Light-polymerized composite resin/Filtek Z250	Bis-GMA, UDMA, BisEMA, initiator (Camphorquinone), 60vol% zirconia/silica	N768474 N868064	
Universal adhesive/Single Bond Universal	Vitrebond copolymer, 10-MDP, silane	527687	3M ESPE,Neuss,Germany
Self-adhesive resin cement/RelyX Unicem	Base paste: methacrylate monomers containing phosphoric acid groups, methacrylate monomers, silanated fillers, initiator components, stabilizers Catalyst paste: methacrylate monomers, alkaline (basic) fillers, silanated fillers, initiator components, stabilizers, pigments	666390	
Universal adhesive/All Bond Universal	10-MDP, Bis-GMA, HEMA, ethanol, water, initiators	1700006050	Bisco Inc., Schaumburg, IL,USA
Porcelain etchant (9.5%)	Hydrofluoric acid, polysulfonic acid	1700002719	
Porcelain primer	Silane	1700003865	
Self-adhesive resin cement/Clearfil SA Luting	Bis-GMA, TEGDMA, 10-MDP, Dimethacrylate, Silanated barium glass filler, Silanated colloidal silica, di-Camphorquinone, Benzoyl peroxide, Initiator, Accelerators	320089	Kuraray Noritake Medical Inc.,Okayama, Japan

Abbreviations: TEGDMA (triethyleneglycol dimethacrylate); Bis-GMA (bisphenol A glycidyl dimethacrylate);UDMA(urethanethyl dimethacrylate); BisEMA(Bisphenol-polyethylene glycol dimethacrylate); 10-MDP (10-methacryloyloxydecyl dihydrogen phosphate);HEMA (hydroxyethyl methacrylate).

Details of materials used for the SBS test are presented in Table 2.

2.3. *XPS and FTIR*

Lithium disilicate blocks were ground into powders. Particles small enough to pass through a 600-mesh sieve were collected. Collected lithium disilicate powders were conditioned with a silane coupling agent, a silane-containg universal adhesive, or a silane-unknown universal adhesive used in the SBS test. After conditioning, the powders were ultrasonically cleaned in acetone for 10 min and centrifuged for 10 min. Sediments were separated and dried at 80 °C. Cleaning and drying procedures were repeated five times.

Lithium disilicate powders conditioned by the silane coupling agent or universal adhesives were examined using FTIR and XPS, with untreated lithium disilicate powders as the control.

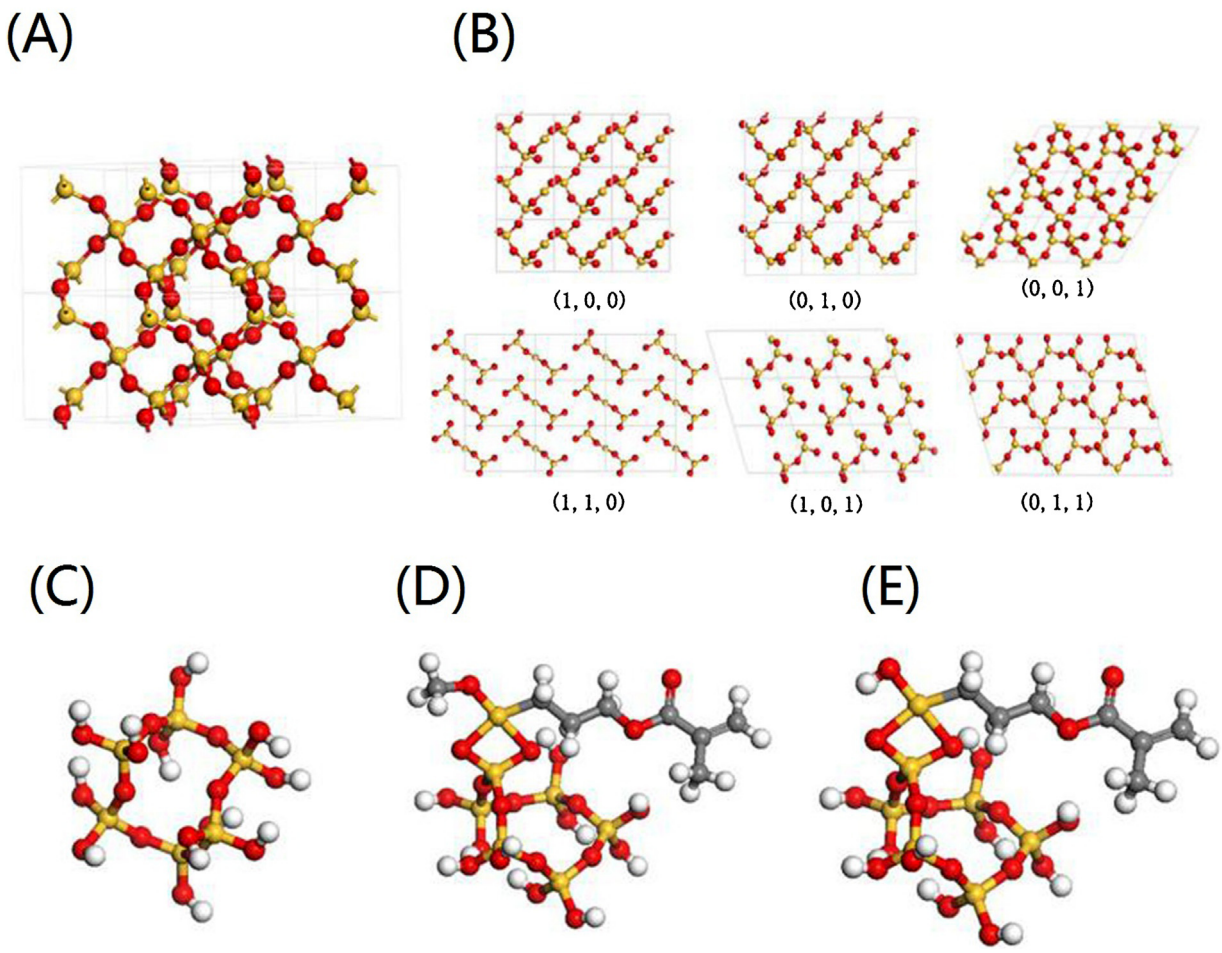

Fig. 1 – γ-MPS and SiO_2 and their complex models built for calculations (A) 2 × 2 unit cell of SiO_2 crystal. (B) Low index faces of SiO_2 crystal. (C) SiO_2 cluster used in DFT calculation. (D) Structure of the γ-MPS-SiO_2 system of incomplete hydrolysis. (E) Structure of the γ-MPS-SiO_2 system of total hydrolysis.

Analyses with FTIR (Nicolet 6700, Thermo Fisher Scientific, Waltham, MA, USA) were performed in the transmission mode by using the KBr pellet technique. Scans were recorded from 4000 to 400 cm^{-1}. The 1800–700 cm^{-1} wavenumber range was defined as the region of interest.

Analyses with XPS (Escalab 250xi, Thermo Fisher Scientific) were conducted using monochromatized A1Kα radiation (1486.6 eV photo energy, energy step size 0.05 eV). Peak fitting was performed using the XPSPeak 4.1 software, and a Shirley function was used to subtract the background. The Lorentzian–Gaussian ratio (L/G ratio) was fixed at 80%.

Table 3 – Thermodynamic calculations of the chemical coordination among γ-MPS, SiO_2 and 10-MDP.

	ΔG(Hartree)	ΔG(kJ/mol)	K
Formula (1)	−0.065277	−171.38	1.06×1030
Formula (2)	0.008952	23.50	/
Formula (3)	−0.065696	−172.48	1.66×1030
Formula (4)	0.008414	22.09	/
Formula (5)	−0.007871	−20.67	4.17×10^3
Formula (6)	−0.005705	−14.98	4.21×10^2

ΔG: change in Gibbs free energy; K: equilibrium constant.

3. Results

3.1. *Complex of γ-MPS and SiO_2 clusters*

Fig. 1A shows the SiO_2 crystal built, and Fig. 1B shows the selected low indices faces. The "ideal" SiO_2 cluster with most features of SiO_2 crystals was chosen for calculation, and H or O atoms were added for charge balance and to generate bonding sites (Fig. 1C). Fig. 1D and E show complexes of γ-MPS combined with SiO_2 cluster incompletely and completely hydrolyzed, respectively, before optimization.

Formulas for combination of the complex of γ-MPS and the SiO_2 cluster in the water phase are enlisted in Fig. 2. The Gibbs free energy and equilibrium constant of the reactions are shown in Table 3.

To study stability, one should consider the Gibbs free energy of the given formula. Formula 1&3 reacted in the aqueous phase, whereas Formula 2&4 reacted at the interface of the aqueous and solid phases. For Formula 2&4 calculation, we used the vacuum phase thermodynamic data for γ-MPS, the

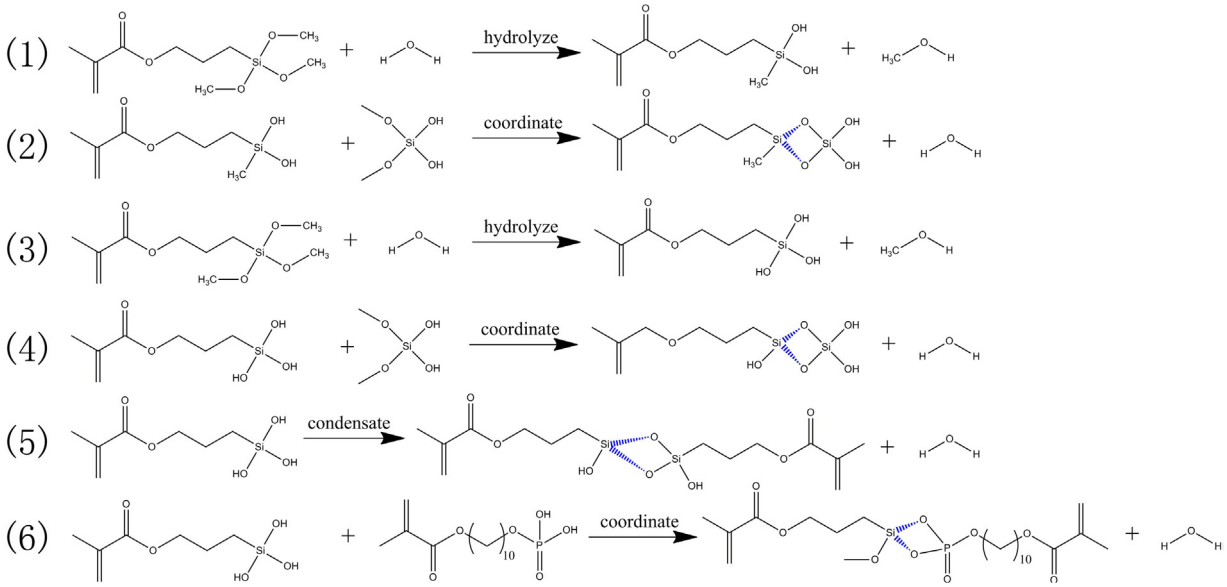

Fig. 2 – (1) Formulas of incomplete hydrolysis of γ-MPS and (2) coordinated with SiO_2. (3) Formulas of total hydrolysis of γ-MPS and (4) coordinated with SiO_2. (5) Formula of dehydration self-condensation of γ-MPS. (6) Formula of 10-MDP coordinated with γ-MPS.

SiO_2 cluster, and their complex because we were only interested in the net binding energy of the reaction at the interface. The solvation effect was not obvious when the head group approached the SiO_2 crystal face because only the hydrophobic hydrocarbon chain was in contact with the aqueous phase. However, the generated H_2O molecule could leave the interface and incur a solvation effect.

According to thermodynamics data, the final Gibbs free energy of Formula 1&2 was −147.88 kJ/mol and that of Formula 3&4 was −150.39 kJ/mol. The final equilibrium constants of Formulas 1&2 and 3&4 were 8.11×10^{25} and 2.24×10^{26}, respectively. Detailed thermodynamic results are included in the *Supporting Information*.

3.2. *Hydrolysis and dehydration self-condensation of γ-MPS*

Formulas of hydrolysis and dehydration self-condensation of γ-MPS are listed in Fig. 2. Dimeric precipitate was calculated as an example to determine whether condensation of γ-MPS can react spontaneously.

According to thermodynamics data listed in Table 3, the Gibbs free energy of Formula 3&5 was −193.15 kJ/mol. The final equilibrium constant was 6.92×10^{33}.

3.3. *Complex of γ-MPS and 10-MDP*

The formula for combination of the complex of γ-MPS and 10-MDP in the water phase is listed in Fig. 2.

According to thermodynamics data listed in Table 3, the final Gibbs free energy of Formula 3&6 was −187.46 kJ/mol. The final equilibrium constant was 6.98×10^{32}.

3.4. *SBS test*

Two-way ANOVA and post-hoc test of SBS data revealed that SBS was significantly affected by surface treatments and aging ($P < 0.01$), while there were no significant interactions between surface treatments and aging ($P = 0.312$).

Fig. 3A showed the means and standard deviations (SDs) of SBS values of all the 10 groups. Regardless of aging being performed or not, the control group (1), wherein no silane-containing product was used, presented the lowest mean SBS, and groups (2, 3, 4, 5, 6, 7, 8, 9 and 10) where silane coupling agent, self-adhesive resin cements, and universal adhesives were used, in combination or alone, yielded higher SBS; however, no significant differences were noted between the group 6, wherein a silane coupling agent was used alone, and group 2, 3, 4 and 5, wherein self-adhesive resin cements or universal adhesives were used alone. Pre-silanization combined with application of self-adhesive resin cements or universal adhesives (7, 8, 9 and 10) provided higher SBS compared with group 2, 3, 4, 5 and 6.

Thermocycling and water storage significantly decreased SBS ($P < 0.05$) in all groups except group 1, 5, 6 and 10. Group 7, 8, 9 and 10 presented similar SBS values either before or after thermocycling and water storage.

Fig. 3B presents the mode of failure analysis. Specimens of most groups showed mixed failure modes, while the group 1 presented 21.4% adhesive fractures after aging.

3.5. *XPS*

The XPS spectra are presented in Fig. 4. Peaks located at the binding energy of 102.68, 102.80, and 102.73 eV in groups using silane coupling agent, silane-containing adhesive, and silane-unknown adhesive, respectively, were assigned as Si—O bond, which were lower than 102.95 eV of the control group.

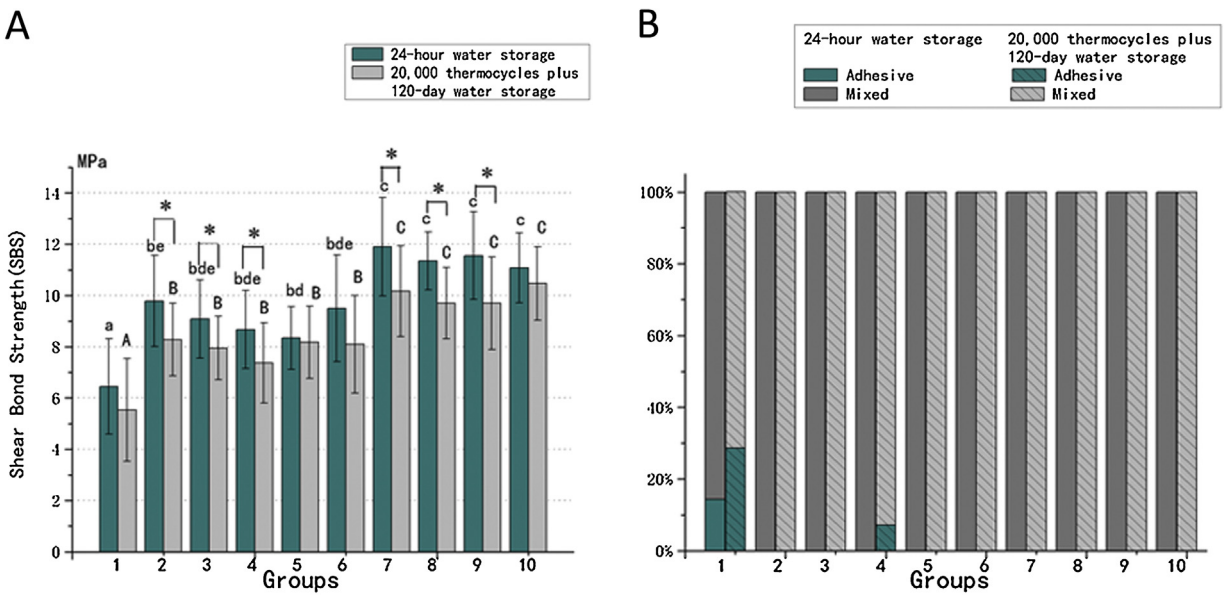

Fig. 3 – (A) Means and standard deviation SBS values of all 10 groups. (B) Failure modes observed in groups of SBS. *Indicates that SBS values were significantly different between 24-h water storage and after aging ($P < 0.05$).

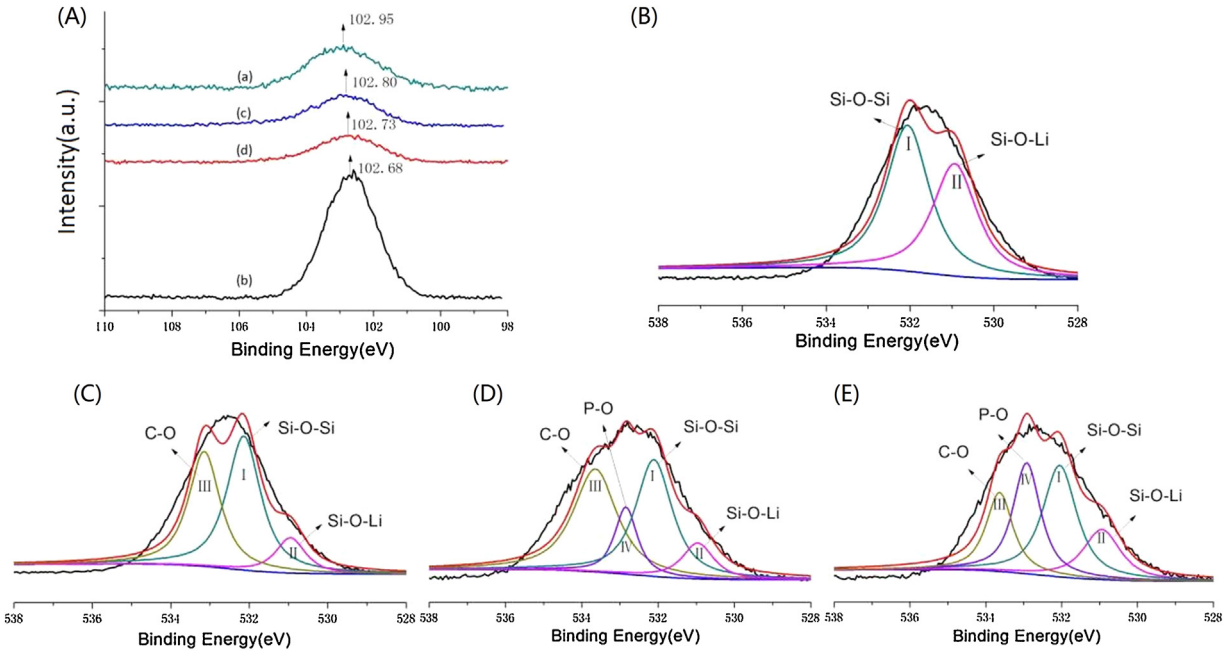

Fig. 4 – (A) X-ray photoelectron spectroscopy Si2p spectra (A) of lithium disilicate powders (a) conditioned with silane coupling agent (b), Single Bond Universal (c), and All Bond Universal (d). X-ray photoelectron spectroscopy O1s spectra oflithium disilicate powders (B) conditioned with silane coupling agent (C), Single Bond Universal (D), and All Bond Universal (E). I ($O_{Si–O–Si}$), II ($O_{Si–O–Li}$), III ($O_{C–O}$), and IV ($O_{P–O}$) represent the four de-convoluted peaks within the main peak. Peak of the Si—O bond downshifted from 102.95 eV in lithium disilicate powders without conditioning to 102.80, 102.73, and 102.68 eV in lithium disilicate powders conditioned by silane-containing adhesive, silane-unknown adhesive, and silane coupling agent, respectively. Peak area ratio of the Si—O—Si bond to the Si—O—Li bond increased progressively from lithium disilicate powders without conditioning to silane-containing adhesives-conditioned lithium disilicate powders, silane-known adhesives-conditioned lithium disilicate powders, and silane coupling agent-conditioned lithium disilicate powders, indicating generation of additional Si—O—Si bonds.

Table 4 – Binding energy of $O_{Si-O-Si}$, $O_{Si-O-Li}$, O_{C-O}, O_{P-O} and relative percentages of $O_{Si-O-Si}/O_{Si-O-Li}$ bond.

Group	Binding energy (eV)				Percentage[a]		Ratio[b]
	Si—O—Si	Si—O—Li	C—O	P—O	Si—O—Si	Si—O—Li	
O	532.1	530.9	–	–	55.72%	44.28%	1.26
Si	532.1	531.0	533.2	–	48.97%	11.35%	4.32
AU	532.1	530.9	533.6	532.9	34.95%	17.29%	2.02
SU	532.1	531.0	533.7	532.8	37.45%	9.87%	3.79

[a] Percentage of each peak was calculated from the relative peak area in the O1s narrow scan XPS spectrum.
[b] Ratio of Si—O—Si/Si—O—Li.

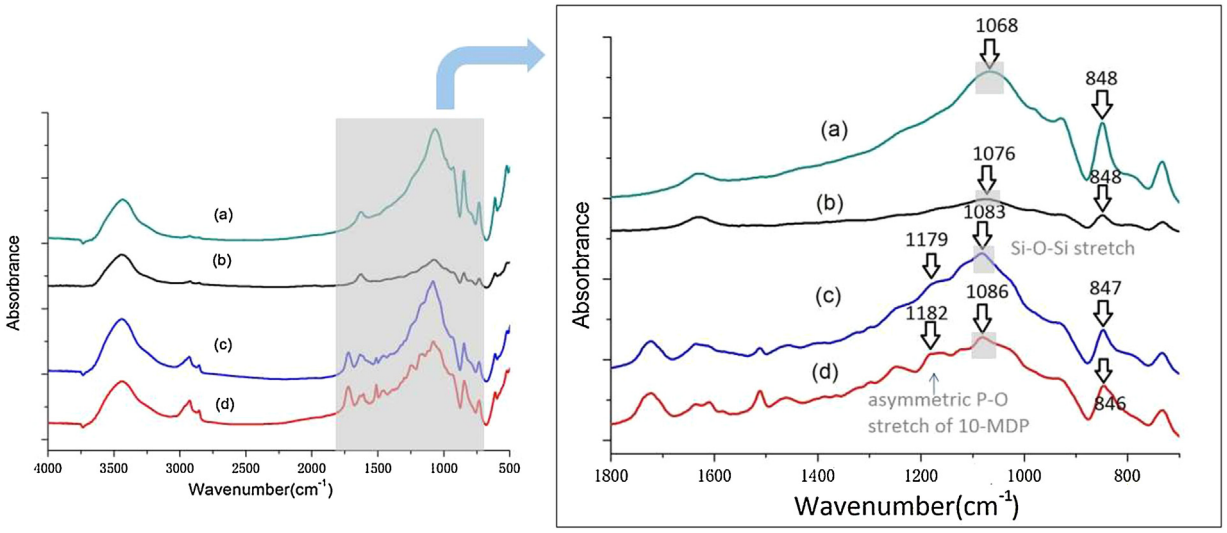

Fig. 5 – Fourier transform infrared spectroscopy absorbance spectra of (a) lithium disilicate powders conditioned with (b) silane coupling agent, (c) Single Bond Universal, and (d) All Bond Universal. The peak from 1068 to 1086 cm^{-1} can be attributed to asymmetric stretching mode of the Si—O—Si bond, and the band around the 847 cm^{-1} region can be attributed to the Si—O—Si bond bending stretching vibration. The peak of symmetric P—O stretch of the PO32– group of 10-MDP was at 1179 and 1182 cm^{-1} in lithium disilicate powders conditioned by silane-containing adhesives and silane-unknown adhesives, respectively.

It suggested that lithium disilicate powders conditioned with both silane coupling agent and universal adhesives generated newly formed Si—O bonds; moreover, more Si—O bonds were observed in silane coupling agent-conditioned lithium disilicate powders.

Narrow-scan spectrum of the O1s region was decomposed into four contributions, identified by peak-fitting procedures in the silane-containing adhesive (Single Bond Universal), silane-unknown adhesive (All Bond Universal), or silane coupling agent (Procelain Primer)-conditioned lithium disilicate powders (Fig. 4B–E). The peak located at 532.1 eV was characteristic of the Si—O—Si bond [15], which was detected in all conditioned lithium disilicate powders as well as lithium disilicate powders without conditioning. The peak located at 530.9 eV in the lithium disilicate powders without conditioning may be attributed to the Si—O—Li bond [16]. Furthermore, peaks at 533.7 and 533.6 eV in lithium disilicate powders conditioned with both silane-containing and silane-unknown adhesives represented the C—O bond [17], and peaks at 532.8 and 532.9 eV are derived from the P—O—H bond [17,18], which should come from 10-MDP in adhesives. Binding energy of the C—O bond that appeared in the silane coupling agent-conditioned lithium disilicate powders was 533.2 eV. Binding energies of each peak are enlisted in Table 4. Because the Si—O—Li bond in lithium disilicate was considered not to react with silane coupling agent or adhesives, the peak area ratios of the Si—O—Si bond to the Si—O—Li bond, which were 1.26, 4.32, 3.79, and 2.02 for lithium disilicate powders without conditioning, silane coupling agent-conditioned lithium disilicate powders, lithium disilicate powders conditioned with silane-containing (Single Bond Universal) and silane-unknown (All Bond Universal) adhesives, respectively, indicate that silane coupling agent-conditioned lithium disilicate powders generated the most Si—O—Si bonds, followed by Single Bond Universal and All Bond Universal.

3.6. FTIR

Fig. 5 shows infrared spectra for lithium disilicate powders irrespective of conditioning. According to Hooshmand et al. the band located around 1087 cm^{-1} can be attributed to the asymmetric stretching mode of the Si—O—Si bond [19]. As observed in Fig. 5, peaks of the Si—O—Si bond changed with addition of a silane coupling agent or a universal adhesive.

Peak of the Si—O—Si bond was at 1068 cm^{-1} in the control group, while it was at 1076, 1083, and 1086 cm^{-1} in lithium disilicate powders conditioned with silane coupling agent, Single Bond Universal, and All Bond Universal, respectively. The band around the 850 cm^{-1} region could be assigned to the Si—O—Si bond bending stretching vibration.

In groups wherein universal adhesives were used, the peak at 1179 and 1182 cm^{-1} represented characteristic peaks of PO_3^{2-} groups, attributed to asymmetric P—O stretch of the molecule of 10-MDP, which was approximately 1085 cm^{-1} according to Suzuki et al. [20]

The absorption peak of Si—OH near 902 cm^{-1} found in lithium disilicate powders conditioned with silane coupling agents or Single Bond Universal that contains silane [6] cannot be detected by FTIR unexpectedly, which suggests that silanol groups in silane coupling agents or Single Bond Universal had been consumed after exposing to lithium disilicate powders.

4. Discussion

The present study investigated four multipurpose products, including two universal adhesives and two self-adhesive resin cements. All these multipurpose products achieved higher bond strength and durability compared with the control group, and bonding improvement was not inferior to bond strength and durability when silane was used alone for bonding silica-based ceramics. This result indicates that it is viable to use these multipurpose products without pre-silanization in clinical practice.

Two factors may influence the bond effectiveness of lithium disilicate: micromechanical retention and chemical bonds [5]. Etching with HF followed by the application of silane coupling agent is the most commonly used bonding strategy [21]. Since the same HF etching was applied, bonding improvement could indeed be attributed to the chemical bonds. Of the four multipurpose products, except Single Bond Universal that is known to contain silane, no product description or studies support that the other three products contain silane. Therefore, we cannot exclude the possibility that bonding improvement resulted from other unknown functional components when the other three products were used for bonding silica-based ceramics. Therefore, XPS and FTIR were conducted to explore chemical reactions between these products and lithium disilicate.

According to FTIR analysis, transformation of the Si—OH bond to the Si—O—Si bond was detected in groups where silane coupling agent and silane-containing universal adhesives were used, indicating the possibility of chemical reactions between silica and silane. Peak of the Si—O—Si bond moved toward a higher wavenumber when a lithium disilicate powder was applied with silane coupling agent or universal adhesives, suggesting that the stretching force constant of the Si—O—Si bond increased and the bond strength enhanced, which could be related to the formation of numerous new chemical bonds. XPS results found similar binding energies of Si2p in groups wherein silane coupling agent, silane-containing universal adhesive, and silane-unknown universal adhesive were used. It changed from relative high binding energy of untreated ceramic powder to a lower one, and the lowest one was detected in the silane coupling agent-using group. Owing to generation of silanol by silane hydrolysis, the Si—O—Si bond was formed between silane and silica [3,6]. Si atoms with lower electronegativity replaced H atoms, increasing the cloud density around Si and O atoms, leading to enhancement of the electronic shielding effect and reduction of binding energy [22]. Similar chemical bond transformation indicates that such silane-unknown adhesives may contain components like silane. XPS O1s spectra concluded similar results: the most Si—O—Si bonds were formed between silane coupling agent and lithium disilicate powders, which can also be generated for the two types of universal adhesives conditioned ceramic powders, suggesting that silane create a chemical bond with silica.

Previous studies have reported that hydrolysis silane in universal adhesives may undergo dehydration condensation [4,5], which can reasonably explain the XPS results that universal adhesive-conditioned lithium disilicate produced less Si—O—Si bonds compared with silane coupling agent. Furthermore, both FTIR and XPS results presented differences regarding lithium disilicate when universal adhesives or silane coupling agents were used alone, indicating the possibility of insufficient active silane contents in multipurpose products or interference by other components. However, the present SBS test showed different results for similar bond effectiveness when using universal adhesives alone compared with using silane coupling agent alone. The present quantum chemistry method was designed to offer the explicit theoretical support to the chemical reaction pathways between silane and silica.

Based on thermodynamic results, actual chemical condensation occurred after thermal activation, leading to siloxane bridges [13]. The self-condensation of γ-MPS reacted most easily, followed by the reaction between γ-MPS and 10-MDP and formation of the siloxane bridges. Hydrolysis of γ-MPS was divided into complete and incomplete hydrolysis based on the pH value as silane hydrolysis is slow in water while acetic acid is commonly used as a reaction catalyst [6]. Yao found that 10% γ-MPS with 10-MDP changed into R-Si(OH)3 in 2 h and siloxane bridge in 10 days by NMR [7]. At the beginning, abundant protons replaced —OCH3 in γ-MPS step by step, such as Formula 1&3 in Fig. 2. Subsequently, the precipitates reacted with silica, forming chemical bonds, and increased the bond strength.

Functional monomers such as γ-MPS and 10-MDP have been retained within the multipurpose products and maintain chemical balance. Although an acidic environment forms around γ-MPS owing to release H^+ of 10-MDP, addition of extra γ-MPS into this balance system or consuming the original γ-MPS of this balance system exposed to silica can be considered as triggers to break the balance, leading to hydrolysis of γ-MPS to generate active silanol groups. Herein γ-MPS in acidic multipurpose products presents instability, which, in turn, induced self-condensation of γ-MPS and interaction between γ-MPS and 10-MDP. Nevertheless, the amount of silanol produced would not had increased if the protons had run out and the dissociation and hydrolysis had reached a new balance. The protons kept descending so that the rate of hydrolysis slowed down and the pH increased. It is difficult for 10-MDP to release H^+ under acidic circumstances [14], making ion exchange between 10-MDP and γ-MPS more challenging, which is why

we supposed that 10-MDP had a less-essential influence in the reaction. Nevertheless, self-condensation of γ-MPS or reaction of γ-MPS with 10-MDP consumed the active silanol, leading to reduction of bonding strength. Pre-silanization will obviously not be affected by chemical environment, thus further enhancing bonding improvement of multipurpose products to lithium disilicate. The present SBS results proved further enhancement of the bond effect when pre-silanization was performed before using multipurpose products. The current SBS test results also showed that thermocycle and water storage decreased SBS in most groups. Although SBS of the group 1, 5, 6 and 10 did not decline significantly, on the basis of the decreasing trend of SBS, we cannot exclude the possibility that detecting minor changes is challenging on account of low sensitivity of the SBS test and larger SDs between samples. No matter before and after artificial aging, several adhesive failure specimens appeared in the control group and Clearfil SA Luting singly used group that received no pre-silanization. Differently, pure mixed failure modes were found both before and after artificial aging in groups that pre-silanization was performed, indicating that pre-silanization improved the bond durability. In addition, despite the SBS results that bond effectiveness based on silanization may be declined by water, it is important to realize that SBS was not only higher in all multipurpose product groups when combined with pre-silanization, although it may have been decreased after aging, but also remained higher compared with groups wherein these multipurpose products were used alone after aging. This also suggests that pre-silanization before using these multipurpose products could be beneficial in clinical practice.

5. Conclusions

Based on the present study, and within its limitations, all null hypotheses can be accepted, and following conclusions may be drawn:

Pre-silanization will further enhance bond improvement of universal adhesives or self-adhesive resin cements when bonded to lithium disilicate. This was because bonding improvement of silane to lithium disilicate can be attributed to hydrolysis of silane to silanol and formation of a Si—O—Si bond between silane and silica. However, in multipurpose products, after hydrolysis of silane to silanol, apart from reacting with silica, silanol also undergoes self-dehydrate condensation or condensation with phosphate monomer 10-MDP. The condensation reaction between silanol and 10-MDP is irreversible and has a negative effect on the formation of siloxane.

Acknowledgments

The authors thank Mr. Taoran Ma and Dr. Hao Wang (Kuraray CO, LTD) for providing Clearfil SA Luting. This work was supported by the National Natural Science Foundation of China [grant number 81400539]; the National Key Research and Development Program of China [grant number 2016YFA0201704]; the Natural Science Foundation of Jiangsu Province [grant numbers BK20150998, BK20140913]; and the Jiangsu Higher Education Institutions [grant number 2018-87].

Appendix A. Supplementary data

Supplementary data associated with this article can be found, in the online version, at https://doi.org/10.1016/j.dental.2019.01.010.

REFERENCES

[1] Piwowarczyk A, Lauer HC, Sorensen JA. In vitro shear bond strength of cementing agents to fixed prosthodontic restorative materials. J Prosthet Dent 2014;92:265–73.
[2] Maruo Y, Nishigawa G, Yoshihara K, Minagi S, Matsumoto T, Irie M. Does 8-methacryloxyoctyl trimethoxy silane (8-MOTS) improve initial bond strength on lithium disilicate glass ceramic. Dent mater 2017;33:e95–100.
[3] Matinlinna JP, Lung CYK, Tsoi JKH. Silane adhesion mechanism in dental applications and surface treatments: a review. Dent Mater 2018;34:13–28.
[4] Lung CY, Matinlinna JP. Aspects of silane coupling agents and surface conditioning in dentistry: an overview. Dent Mater 2012;28:467–77.
[5] Matinlinna JP, Vallittu PK. Bonding of resin composites to etchable ceramic surfaces — an insight review of the chemical aspects on surface conditioning. J Oral Rehabil 2007;34:622–30.
[6] Yoshihara K, Nagaoka N, Sonoda A, Maruo Y, Makita Y, Okitara T, et al. Effectiveness and stability of silane coupling agent incorporated in 'universal' adhesives. Dent Mater 2016;32:1218–25.
[7] Yao C, Yu J, Wang Y, Tang C, Huang C. Acidic pH weakens the bonding effectiveness of silane contained in universal adhesives. Dent mater 2018;34:809–18.
[8] Kim RJY, Woo JS, Lee IB, Yi YA, Hwang JY, Seo DG. Performance of universal adhesives on bonding to leucite-reinforced ceramic. Biomater Res 2015;19:11.
[9] Hitz T, Stawarczyk B, Fischer J. Are self-adhesive resin cements a valid alternative to conventional resin cements? A laboratory study of the long-term bond strength. Dent Mater 2012;28:1183–90.
[10] Peumans M, Valjakova EB, De Munck J, Mishevska CB, Van Meerbeek B. Bonding Effectiveness of Luting Composites to Different CAD/CAM Materials. J Adhes Dent 2016;18:289–302.
[11] Antonucci J, Dickens S, Fowler B, Xu HHK, McDonough WG. Chemistry of silanes: interfaces in dental polymers and composites. J Res Natl Inst Stand Technol 2005;110:541–58.
[12] Van HE, Weckhuysen B. Phosphorus promotion and poisoning in zeolite-based materials: syntesis, characterization and catalysis. Chem Soc Rev 2015;44:7406–28.
[13] Salon MC, Abdelmouleh M, Boufi S, Belgacem MN, Gandini A. Silane adsorption onto cellulose fibers: hydrolysis and condensation reactions. J Colloid Interf Sci 2005;289:249–61.
[14] Xie H, Tay FR, Zhang F, Lu Y, Shen S, Chen C. Coupling of 10-methacryloyloxydecyldihydrogenphosphate to tetragonal zirconia: Effect of pH reaction conditions on coordinate bonding. Dent Mater 2015;31:e218–25.
[15] Araujo YC, Toledo PG, Leon V, Gonzalez HY. Wettability of silane-treated glass slides as determined from X-ray photoelectron spectroscopy. J Colloid Interf Sci 1995;176:485–90.
[16] Soares PC, Nascente PAP, Zanotto ED. XPS study of lithium disilicate glass crystallisation. Phys Chem Glasses B 2002;43:143–6.

[17] Lin XZ, Yuan ZY. Synthesis of amorphous porous zirconium phosphonate materials: tuneable from micropore to mesopore sizes. RSC Adv 2014;4:32443–50.
[18] Adolphi B, Jahne E, Busch G, Cai X. Characterization of the adsorption of omega-(thiophene-3-yl alkyl) phosphonic acid on metal oxides with AR-XPS. Anal Bioanal Chem 2004;379:646–52.
[19] Hooshmand T, van NR, Keshvad A. Storage effect of a pre-activated silane on the resin to ceramic bond. Dent Mater 2004;20:635–42.
[20] Suzuki M, Fujishima A, Miyazaki T, Hisamitsu H, Ando H, Nakahara M, et al. A study on adsorption structures of methacryloyloxyalkyl dihydrogen phosphates on silver substrates by infrared reflection absorption spectroscopy. J Biomed Mater Res 1997;37:252–60.
[21] Meng HL, Xie HF, Yang L, Chen BZ, Chen Y, Zhang HQ, et al. Effects of multiple firings on mechanical properties and resin bonding of lithium disilicate glass-ceramic. J Mech Behav Biomed 2018;88:362–9.
[22] Wang F, Feng Q, Wang W, Huang Y. Surface modification of ultrafine silica powder with silane coupling agent KH550. Mater Rev 2014;28:70–3.